

Search for the Standard Model Higgs boson Decaying to ZZ at CMS

Gurpreet Singh*

On behalf of the CMS Collaboration

Universita Degli Studi di Bari, Aldo Moro, Piazza Umberto I, Bari, Italy, 70121

Istituto Nazionale di Fisica Nucleare - Sezione INFN di Bari, Bari, Italy, 70125

E-mail: gurpreet.singh@cern.ch

A search for the standard model Higgs boson decaying to ZZ is presented by using the proton-proton collision data recorded by the CMS experiment during year 2011 and 2012 at centre-of-mass energies 7 TeV and 8 TeV. Four sub-channels are presented in accord with further decay modes of Z bosons as $H \rightarrow ZZ \rightarrow 4\ell$, $H \rightarrow ZZ \rightarrow 2\ell 2\tau$, $H \rightarrow ZZ \rightarrow 2\ell 2\nu$ and $H \rightarrow ZZ \rightarrow 2\ell 2\text{jets}$. A new boson is observed with a local significance above the expected background of 4.5 standard deviations in the context of the $H \rightarrow ZZ \rightarrow 4\ell$ decay channel. The signal strength μ , relative to the expectation for the standard model Higgs boson, is measured to be $\mu = 0.80^{+0.35}_{-0.28}$ at 126 GeV. The measured mass in the ZZ channel, where both Z bosons decay to e or μ pairs, is 126.2 ± 0.6 (stat) ± 0.2 (syst) GeV. The angular distributions of the lepton pairs in this channel are sensitive to the spin-parity of the boson. Under the assumption of spin 0, the present data are consistent with the pure scalar hypothesis, while disfavoring the pure pseudoscalar hypothesis.

*International Winter Meeting on Nuclear Physics,
21-25 January 2013
Bormio, Italy*

*Speaker.

1. Introduction

An important goal of the LHC physics program is to ascertain the mechanism of electroweak symmetry breaking, through which the W and Z bosons acquire mass. In the standard model (SM), this is achieved via the Higgs mechanism, where electroweak interactions rely on the existence of the Higgs boson (H, with mass m_H), a scalar particle associated with the field responsible for the spontaneous electroweak symmetry breaking.

For Higgs masses heavy enough to energetically allow the decay to pairs of electroweak vector bosons, these decay channels are the ones dominating the search strategies. According to further decay modes of Z bosons, four decay chains drive the effort: the ‘golden’ fully leptonic final state ($H \rightarrow ZZ \rightarrow 4\ell$), $H \rightarrow ZZ \rightarrow 2\ell 2\tau$, the leptonic final state with neutrinos ($H \rightarrow ZZ \rightarrow 2\ell 2\nu$) and the semileptonic one ($H \rightarrow ZZ \rightarrow 2\ell 2\text{jets}$). Here and henceforward, letter ‘ ℓ ’ is to be understood as electron or muon. Compared to the golden leptonic decay channel, the two latter final states benefit from more favorable branching ratios, so that their effective cross section is, respectively, about 6 and 20 times larger than the golden channel. On the other hand, the intrinsic complexity of jet and missing transverse energy reconstruction, as well as the higher level of expected backgrounds, pose more demanding experimental challenges to these analyses.

In July 2012, the CMS and ATLAS experiments announced [1, 2] the discovery of a new boson at a mass around 125 GeV, with properties compatible with the SM Higgs boson. The properties examined are the signal strength, relative to the expectation for the SM Higgs boson, the mass, the parity quantum number, and the corresponding fraction of a CP-violating contribution to the decay amplitude expressed through the fraction of the decay rate.

2. The $H \rightarrow ZZ \rightarrow 4\ell$ and $H \rightarrow ZZ \rightarrow 2\ell 2\tau$ Analysis

A comprehensive search for the SM Higgs boson is performed over the $H \rightarrow ZZ \rightarrow 4\ell$ and $H \rightarrow ZZ \rightarrow 2\ell 2\tau$ channels [3] by using 5.1 fb^{-1} of pp collision data from the CMS experiment [4] collected in 2011 at $\sqrt{s} = 7 \text{ TeV}$, and 12.2 fb^{-1} collected in 2012 at $\sqrt{s} = 8 \text{ TeV}$. The $H \rightarrow ZZ \rightarrow 4\ell$ decay channel is often called the ‘golden channel’ due to its clean experimental signature of four isolated leptons, electrons or muons. The analysis presented in this paper relies critically on the reconstruction, identification, and isolation of leptons. The high lepton reconstruction efficiencies are achieved for a ZZ system composed of two pairs of same-flavour and opposite-charge isolated leptons, ($e^\pm e^\pm$, $\mu^\pm \mu^\pm$), or $\tau^\pm \tau^\pm$, in the measurement range $m_{4\ell}, m_{2\ell 2\tau} > 100 \text{ GeV}$. One or both of the Z bosons can be off-shell. The single-resonant four-lepton production ($Z \rightarrow 4\ell$) is used as a standard candle in the mass range $70 < m_{4\ell} < 100 \text{ GeV}$. The background sources include an irreducible four-lepton contribution from direct ZZ (or $Z\gamma^*$) production via $q\bar{q}$ annihilation and gg fusion. Reducible contributions arise from $Zb\bar{b}$ and $t\bar{t}$ where the final states contain two isolated leptons and two b jets producing secondary leptons. Additional background of instrumental nature arises from Z + jets and WZ + jets events where jets are misidentified as leptons.

The signal candidates in the 4ℓ analysis are selected with four isolated leptons, electrons or muons. The electrons are reconstructed within $\eta < 2.5$ and for $p_T > 7 \text{ GeV}$. Muons are reconstructed within $\eta < 2.4$ and for $p_T > 5 \text{ GeV}$. The Z candidates are formed from a pair of leptons of the same flavor and opposite charge. The pair with a reconstructed mass closest to the nominal

Z boson mass (Z_1) is required to satisfy $40 < m_{Z_1} < 120$ GeV. The second Z boson candidates (Z_2) are formed from all remaining leptons and are required to satisfy $12 < m_{Z_2} < 120$ GeV. Keeping in view the small production cross section of the 4ℓ channels, the final state radiation ($Z \rightarrow \ell^+ \ell^- \gamma$) recovery has been applied in signal and background phase spaces. To ensure that selected events have leptons on the high-efficiency plateau for the trigger, at least one lepton is required to have $p_T > 20$ GeV and second $p_T > 10$ GeV. A minimum di-lepton mass requirement of 4 GeV is imposed on all opposite-charge lepton pairs to reduce backgrounds originating from low-mass hadron decays. The phase space for the search of the SM Higgs boson is defined by restricting the mass range to $m_{4\ell} > 100$ GeV. A higher minimal threshold on m_{Z_1} and m_{Z_2} could be used for higher m_H values but only with marginal improvement of the sensitivity.

For the search in the $2\ell 2\tau$ final state, events are required to have one $Z_1 \rightarrow \ell^+ \ell^-$ candidate with one lepton at $p_T > 20$ GeV and the other at $p_T > 10$ GeV, and a $Z_2 \rightarrow \tau^+ \tau^-$, with τ decaying into μ , e or τ_h . The leptons from the τ leptonic decays are required to have $p_T^\ell > 10$ GeV. The τ_h must have $p_T^{\tau_h} > 20$ GeV. The final state radiation recovery is not applied for the $2\ell 2\tau$ final state. The invariant mass of the reconstructed Z_1 is required to satisfy $60 < m_{\ell\ell} < 120$ GeV, and that of the Z_2 to satisfy $m_{\tau\tau} < 90$ GeV. At low $m_{\tau\tau}$, the Z_2 is restricted by the selection requirements on the p_T of the leptons. Thus, the $2\ell 2\tau$ final states contribute only to the ‘‘high-mass’’ part of the analysis ($m_{2\ell 2\tau} > 180$ GeV).

The angular distribution of decay products of the SM Higgs boson is independent of the production mechanism as it’s spinless. Five angles ($\theta, \Phi_1, \theta_1, \theta_2, \Phi$) defined in Ref. [5] and the masses of the lepton pairs, m_{Z_1} and m_{Z_2} , fully describe the decay kinematics of the four-lepton system. These observables provide significant discrimination between signal and background processes in addition to the four-lepton mass. A matrix element likelihood analysis (MELA) is used. A kinematic discriminant (MELA KD = $\mathcal{P}_{sig}/(\mathcal{P}_{sig} + \mathcal{P}_{bkg})$) is constructed based on the probability ratio of the signal and background hypotheses. The likelihood ratio is defined for each value of $m_{4\ell}$.

The ZZ background is evaluated from Monte-Carlo simulation. This includes the dominant process of $q\bar{q}$ annihilation, as well as gluon fusion. To estimate the reducible ($Zb\bar{b}/c\bar{c}$, $t\bar{t}$) and instrumental (Z + light jets, WZ + jets) backgrounds, a Z + X background control region is defined where X consists of two reconstructed leptons, at least one of which is a nonprompt lepton, including misidentified leptons, leptons from heavy-quark decays, or photon conversions. The background is estimated using the probability for a reconstructed object to pass the isolation and identification requirements. The contamination from WZ in these events is suppressed by requiring missing transverse energy below 25 GeV. The lepton misidentification probability is compared, and found compatible, with the one derived from MC simulation.

Two different approaches are used to extrapolate the measured event rates to the signal region. Both start by relaxing the isolation and identification criteria for two additional reconstructed lepton objects. In first approach, the additional pair of leptons is required to have the same charge (to avoid signal contamination) and same flavour ($e^\pm e^\pm$, $\mu^\pm \mu^\pm$), a reconstructed invariant mass $m_{Z_2} > 12$ GeV, and $m_{4\ell} > 100$ GeV. The expected number of Z + X background events in the signal region is obtained by taking into account the lepton misidentification probability for each of the two additional leptons. The second method, used also for $\tau\tau$ final states, employs the control region with two opposite-sign leptons failing the isolation and identification criteria. In addition, a control region with three passing and one failing lepton is also used to account for contributions

from backgrounds with three prompt leptons and one misidentified lepton. The validity of the two methods is assessed with closure tests in the simulation and checks with data on samples using relaxed charge and flavor requirements. Comparable background counts in the signal region are found within uncertainties from both methods. An envelope comprising these results is used as the final estimate in Table 1.

The reconstructed four-lepton invariant-mass distributions for the 4ℓ , combining the $4e$, 4μ , and $2e2\mu$ channels, are shown in Figure 1 (right) and compared with the expectation from SM background processes. The observed distribution is in good agreement with the expectation. The peak of the $Z \rightarrow 4\ell$ candle around $m_{4\ell} = m_Z$ is observed as expected. The measured distribution at higher mass is dominated by the irreducible ZZ background. A clear peak around $m_{4\ell} = 126$ GeV is seen. The reconstructed visible mass distributions for the $2\ell 2\tau$ selection, combining all the $\ell^+\ell^-\tau^+\tau^-$ final states, are shown in Figure 1 (left) and compared to the SM background expectation. The background shapes are taken from MC simulation and the rates are normalised to the values obtained using a method based on data. The measured distribution is well described by the SM background expectation.

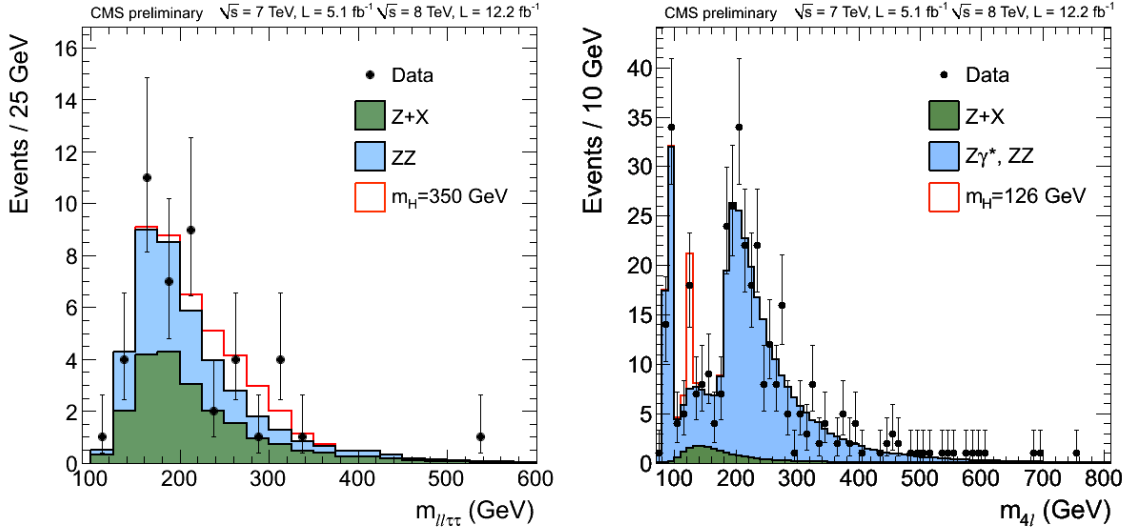


Figure 1: Distribution of the four-lepton reconstructed mass in full mass range for the sum of the $4e$, 4μ , and $2e2\mu$ channels (right), and for the sum over all $\ell^+\ell^-\tau^+\tau^-$ channels (left). Points represent the data, shaded histograms represent the background and unshaded histogram the signal expectations. No event is observed for $m_{4\ell} > 800$ GeV or $m_{2\ell 2\tau} > 600$ GeV.

The number of candidates observed as well as the estimated background are reported in Table 1, for the selection in the full mass measurement range for the SM-like Higgs boson search, $100 < m_{4\ell}, m_{2\ell 2\tau} < 1000$ GeV. The expected number of signal events is also given for several SM-like Higgs boson mass hypotheses. The observed event rates for the various channels are compatible with the SM background expectation. The distributions of the MELA KD versus the four-lepton reconstructed mass ($m_{4\ell}$) is shown for the selected events and compared to the SM background and signal ($m_H = 126$ GeV) expectations in Figure 2. The comparison of the left and the right plot shows the discrimination between signal and background processes.

Table 1: The number of event candidates observed, compared to the mean expected background and signal rates for each final state. The results are given integrated over the full mass measurement range for the SM-like Higgs boson search from 100 to 1000 GeV and for 2011 and 2012 data combined.

Channel	$4e$	4μ	$2e2\mu$	$2\ell 2\tau$
ZZ background	53.0 ± 6.3	82.7 ± 8.9	131.1 ± 14.3	19.0 ± 2.3
Z + X	$7.6^{+6.9}_{-5.2}$	$2.9^{+2.2}_{-1.6}$	$10.1^{+9.9}_{-6.5}$	20.4 ± 6.2
All background expected	$60.7^{+9.3}_{-8.2}$	$85.6^{+9.2}_{-9.1}$	$141.3^{+17.3}_{-15.7}$	39.4 ± 6.6
$m_H = 125$ GeV	2.4 ± 0.4	4.6 ± 0.5	6.0 ± 0.7	–
$m_H = 126$ GeV	2.7 ± 0.4	5.1 ± 0.6	6.6 ± 0.8	–
$m_H = 200$ GeV	15.5 ± 1.9	23.1 ± 2.6	38.5 ± 4.3	5.6 ± 0.6
$m_H = 350$ GeV	9.5 ± 1.2	13.6 ± 1.5	23.2 ± 2.7	5.7 ± 0.6
$m_H = 500$ GeV	3.3 ± 0.4	4.7 ± 0.6	8.1 ± 0.9	2.8 ± 0.3
Observed	59	95	162	45

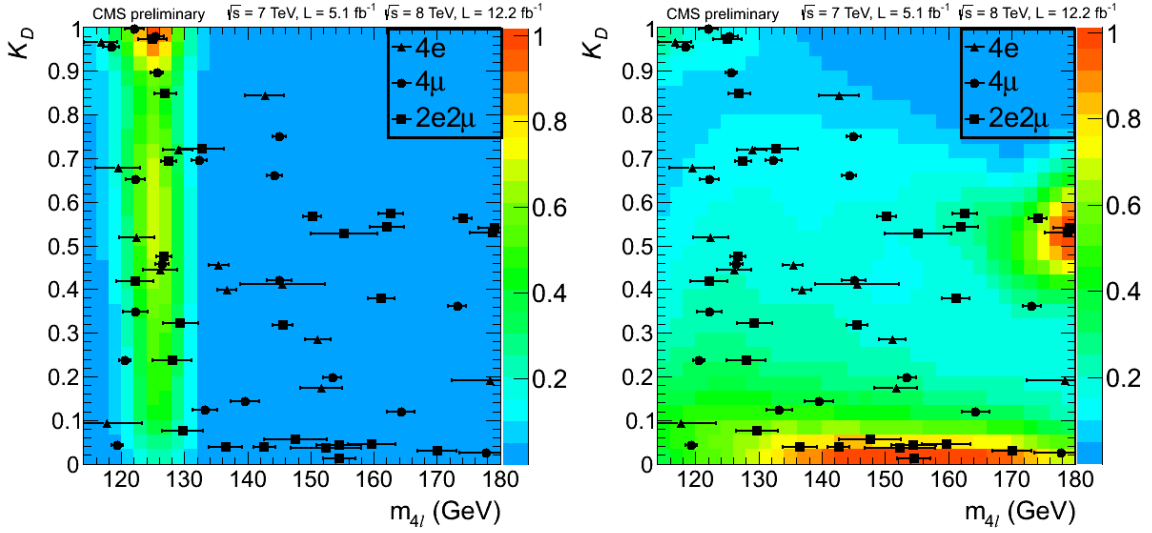


Figure 2: Distribution of the MELA KD versus the four-lepton reconstructed mass $m_{4\ell}$ in the low-mass region. The individual events are shown with their reconstructed mass uncertainties. The contours represent the expected relative density of signal events (left) and background (right).

The upper limits obtained from the combination of the 4ℓ and $2\ell 2\tau$ channels with CLs method [6] are shown in Figure 3 (left). The SM-like Higgs boson is excluded by the four-lepton channels at 95% CL in the ranges 113 – 116 GeV and 129 – 720 GeV. The compatibility of the observed excesses of data events with the background-only hypothesis can be quantified by the p-value. The p-value is the probability of observing an upwards fluctuation of the background event yield at least as large as the one measured in data. The local p-values, representing the significance of local excesses relative to the background expectation, are shown for the full mass range as a function of m_H in Figure 3 (right). The minimum of the local p-value is reached at low mass around $m_{4\ell} = 125.9$ GeV, near the mass of the new boson, and corresponds to a local significance of 4.5σ .

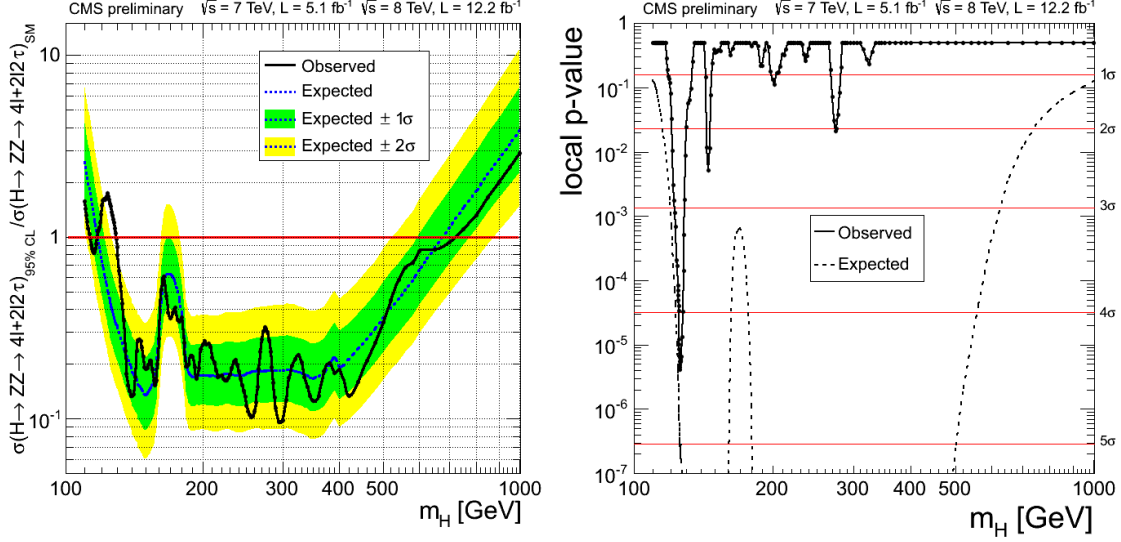


Figure 3: Observed and expected 95% CL upper limit (left) on the ratio of the production cross section to the SM expectation. The 68% and 95% ranges of expectation for the background-only model are also shown with green and yellow bands, respectively. Significance of the local excess (right) with respect to the SM background expectation as a function of the Higgs boson mass in the full mass range from 100 to 1000 GeV.

The signal strength μ , relative to the expectation for the SM Higgs boson, is measured to be $\mu = 0.80^{+0.35}_{-0.28}$ at 126 GeV. The mass measurement of the new resonance is performed with a three-dimensional fit using for each event the four-lepton invariant mass, the associated per-event mass error, and the kinematic discriminant. Figure 4 (left) shows the two-dimensional 68% CL regions for the signal strength μ , relative to the expectation for the SM Higgs boson, versus m_H . A simultaneous fit of the mass and of μ gives $m_H = 126.2 \pm 0.6$ (stat) ± 0.2 (syst) GeV.

The MELA methodology has been used to determine the spin, parity and quantum numbers of the new boson, where instead of signal-to-background probability ratio we construct probability ratio for two signal hypotheses. Figure 4 (right) shows the distribution of $q = -2\ln\mathcal{L}_{0^-} / \mathcal{L}_{0^+}$ with generated samples of background and signal of two types, SM 0^+ and 0^- , for $m_H = 126$ GeV. The expected distributions are generated with signal cross-section equal to that of the SM, which is consistent with observation. We find consistent results when the expected distributions are generated with the measured signal strength. The mean of the expected SM 0^+ distribution is 1.9 standard deviations in the tail of the 0^- distribution, while the mean of the expected 0^- distribution is 2.0 standard deviations in the tail of the 0^+ distribution. The observed value of q , indicated by an arrow in Figure 4 (right), is consistent with expectation, assuming $JP = 0^-$, within 2.4 standard deviations and consistent with expectation, assuming $JP = 0^+$, within 0.5 standard deviations. We define a CLs criterion as the ratio of the probabilities to observe, under the 0^+ and 0^- hypotheses, a value of the test statistics q equal or larger than the one in the data. The data disfavors the pseudoscalar hypothesis 0^- with a CLs value of 2.4%. The distribution of $-2\ln\mathcal{L}$ as a function of f_{a3} and signal strength, μ is also measured. The measurement of the fraction of a CP-violating contribution to the decay amplitude expressed through the fraction of the corresponding decay rate is $f_{a3} = 0.00^{+0.31}_{-0.00}$.

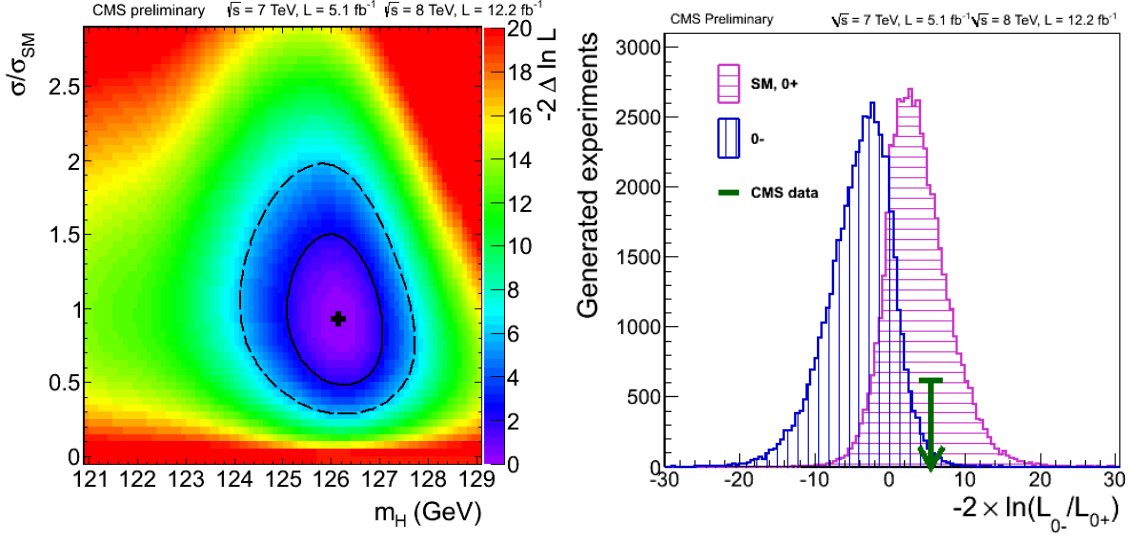


Figure 4: LEFT: Distribution of $-2\ln\mathcal{L}$ as a function mass m_H and signal strength μ . The central point shows the minimum value of $-2\ln\mathcal{L}$, the solid and dashed contours show 68% and 95% CL contours in two dimensions. RIGHT: Distribution of $q = -2\ln\mathcal{L}_{0-}/\mathcal{L}_{0+}$ for two signal types (0^+ horizontally hatched histogram, 0^- vertically hatched histogram) for $m_H = 126$ GeV shown with a large number of generated experiments. The arrow indicates the observed value.

3. The $H \rightarrow ZZ \rightarrow 2\ell 2\nu$ Analysis

The $H \rightarrow ZZ \rightarrow 2\ell 2\nu$ [8, 9] analyses is performed over 5.0 fb^{-1} data collected in 2011 at $\sqrt{s} = 7$ TeV, and 5.0 fb^{-1} collected in 2012 at $\sqrt{s} = 8$ TeV. One of the two Z bosons is required to decay to neutrinos. The kinematics of the final state are not fully known as neutrinos are not reconstructed in the detector. Rather, the presence of the invisible Z decay will manifest as missing transverse energy (E_T^{miss}). A search performed for the resonant production of ZZ pairs via the SM Higgs boson decay by analyzing the spectra of E_T^{miss} and the reconstructed transverse mass (M_T) of the dilepton and E_T^{miss} system. The M_T variable is calculated as follows:

$$M_T^2 = \left(\sqrt{p_T(\ell\ell)^2 + M(\ell\ell)^2} + \sqrt{E_T^{\text{miss}2} + M(\ell\ell)^2} \right) - (\vec{p}_T(\ell\ell) + \vec{E}_T^{\text{miss}})^2 \quad (3.1)$$

Two broad analysis categories are defined as electroweak vector boson fusion (VBF) and gluon fusion. All events failing the VBF selection are considered in gluon fusion category and further divided in accord with the number of reconstructed jets into three additional categories ($N_{jets} = 0, 1$ and 2). In the VBF category, mass-independent requirements are enforced in the form $p_T^Z > 55$ GeV and $E_T^{\text{miss}} > 70$ GeV, whereas in the three gluon fusion categories, optimized, mass-dependent selections on E_T^{miss} and transverse mass M_T are applied.

The reconstructed E_T^{miss} represents the main tool of background discrimination. The dominant background process is constituted by Drell-Yan ($Z \rightarrow \ell\ell$) + E_T^{miss} events, in which the reconstructed E_T^{miss} is originated by instrumental and reconstruction effects. The events having a significant

amount of E_T^{miss} are considered to effectively contrast background processes. A control sample in data has been identified in $\gamma + E_T^{miss}$ because it has similar distributions of instrumental E_T^{miss} as $Z \rightarrow \ell\ell + E_T^{miss}$ events and the larger γ +jet cross section offers greater statistical power. A reweighting procedure is applied, based on the transverse momentum of the boson and the reconstructed vertex multiplicity to have same kinematic properties of $Z + E_T^{miss}$ events. Other notable background processes to this channel are non-resonant dilepton events ($t\bar{t}, WW$) and resonant dilepton events arising from continuous diboson production (ZZ, WZ). The latter are taken from the Monte Carlo simulation. The remaining backgrounds are estimated using control samples in data.

After the full set of event selection requirements is applied, the observed yields in data are compared to the background and signal expectations for different m_H hypotheses in the 200 – 600 GeV range, and interpreted as upper limits on the Higgs boson production cross section with the CLs technique. No evidence found for the SM Higgs boson and results are shown in Figure 5. This channel excludes SM Higgs boson in the $278 < m_H < 600$ GeV range with 95% confidence level.

4. The $H \rightarrow ZZ \rightarrow 2\ell 2\text{jets}$ Analysis

A search for the SM Higgs boson decaying to two Z bosons with subsequent decay to a final state with two leptons and two quark-jets [7], is presented over 4.6 fb^{-1} data collected in 2011 at $\sqrt{s} = 7 \text{ TeV}$. The four-momenta of the four final state decay products of $H \rightarrow ZZ \rightarrow 2\ell 2\text{jets}$ channel are completely reconstructed in the detector therefore a search is performed for an invariant mass peak over a background spectrum. The presence of jets deteriorate the Higgs mass resolution and increase the level of backgrounds. A kinematic fit on the dijet system constrains the dijet invariant mass to the nominal Z boson mass, and does so by fully taking into account the jet energy and angular resolutions as a function of the jet pseudorapidity and transverse momentum, leading to a significant improvement in the expected m_H resolution.

The jet flavor provides a powerful means of background discrimination. Jets in signal events are produced in hadronic decays of a Z boson and originate from the hadronization of quark partons. The dominant background is represented by a leptonically-decaying Z boson produced in association with hard jets, a process in which gluon radiation is expected to play a major role. In

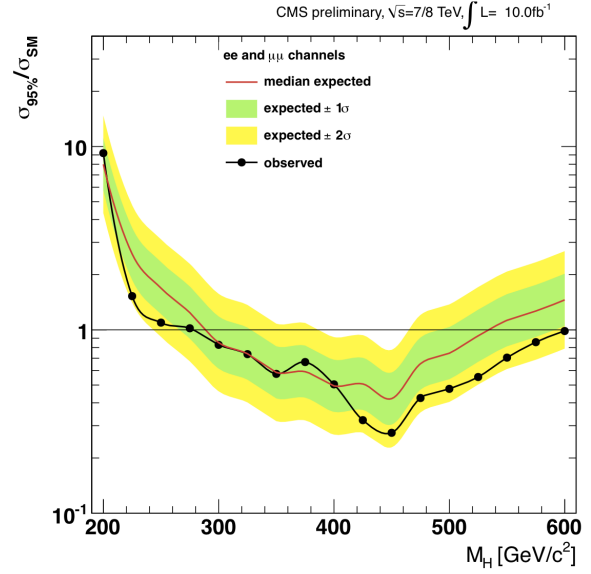


Figure 5: Observed (black) and expected (red) 95% CL upper limit on the ratio of the production cross section to the SM expectation for the Higgs boson obtained using the CLs technique in the $H \rightarrow ZZ \rightarrow 2\ell 2\nu$ analysis. The 68% and 95% ranges of expectation for the background-only model are also shown with green and yellow bands, respectively. The solid line at 1 indicates the SM expectation.

addition to gluons, u and d quarks, valence partons of the protons, dominate the jet production associated with the Z.

The first directive is to isolate the $Z \rightarrow b\bar{b}$ contribution and further categorize the samples in three exclusive categories, depending on the amount of jets (either 0, 1 or 2) in the final state which have been found compatible with the hadronization of a bottom quark (b-tags). The second approach is the use of a likelihood discriminant (LD) which, by studying the particle composition of the reconstructed jets, is able to distinguish between light quark and gluon hadronization. The kinematic discrimination between signal and background is performed through an angular analysis, based on the study presented in Ref. [5].

No evidence for the SM Higgs boson production is observed as shown in Figure 6. The low mass analysis excludes a cross section three times the SM around 155 GeV, whereas the high mass analysis reaches sensitivity to the SM expectation in the 370 – 400 GeV interval.

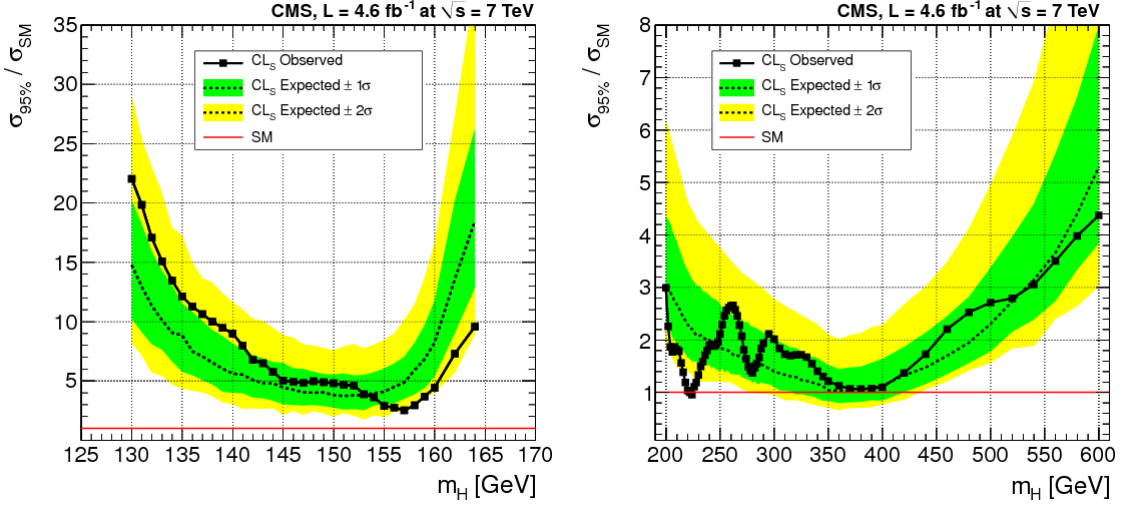


Figure 6: Observed (solid) and expected (dashed) 95% CL upper limit on the ratio of the production cross section to the SM expectation for the Higgs boson obtained using the CLs technique in the $H \rightarrow ZZ \rightarrow 2\ell 2\text{jets}$ analysis. The 68% and 95% ranges of expectation for the background-only model are also shown with green and yellow bands, respectively. Left: low mass range, right: high mass range.

5. Conclusions

The search for the SM Higgs boson decaying to ZZ has been presented. In accord with further decay modes of Z bosons, four sub-channels are analysed as $H \rightarrow ZZ \rightarrow 4\ell$, $H \rightarrow ZZ \rightarrow 2\ell 2\tau$, $H \rightarrow ZZ \rightarrow 2\ell 2\nu$ and $H \rightarrow ZZ \rightarrow 2\ell 2\text{jets}$. The new boson recently discovered by the ATLAS and CMS experiments is observed in the 4ℓ channel, with a local significance of 4.5 standard deviations above the expected background. The mass distributions are measured with four-lepton invariant masses $m_{4\ell} > 100$ GeV using 5.1 fb^{-1} data at $\sqrt{s} = 7$ TeV and 12.2 fb^{-1} at $\sqrt{s} = 8$ TeV. The measurements are interpreted by using information for each event about the measured four-lepton mass, the mass uncertainty, and a kinematic discriminant. Upper limits at 95% confidence

level exclude the SM-like Higgs boson in the ranges 113 – 116 GeV and 129 – 720 GeV while the expected exclusion range is 118 – 670 GeV. The signal strength μ , relative to the expectation for the SM Higgs boson, is measured to be $\mu = 0.80_{-0.28}^{+0.35}$ at 126 GeV. A measurement of its mass gives 126.2 ± 0.6 (stat) ± 0.2 (syst) GeV.

The hypothesis 0^+ of the SM for the spin $J = 0$ and parity $P = +1$ quantum numbers is found to be consistent with the observation. Under the assumption that the observed boson has spin zero, the data disfavor the pseudoscalar hypothesis 0^- with a CLs value of 2.4%. The fraction of a CP-violating contribution to the decay amplitude, expressed through the fraction f_{a3} of the corresponding decay rate, is measured to be $f_{a3} = 0.00_{-0.00}^{+0.31}$, and thus consistent with SM expectation.

References

- [1] CMS Collaboration, “Observation of a new boson at a mass of 125 GeV with the CMS experiment at the LHC”, *Phys. Lett. B* 716 (2012) 30-61.
doi:10.1016/j.physletb.2012.08.021, arXiv:1207.7235.
- [2] ATLAS Collaboration, “Observation of a new particle in the search for the Standard Model Higgs boson with the ATLAS detector at the LHC”, *Phys. Lett. B* 716 (2012) 1-29.
doi:10.1016/j.physletb.2012.08.020, arXiv:1207.7214.
- [3] CMS Collaboration, “Updated results on the new boson discovered in the search for the standard model Higgs boson in the $H \rightarrow ZZ^* \rightarrow 4\ell$ channel in pp collisions at $\sqrt{s} = 7$ and 8 TeV”, CMS-PAS-HIG-12-041.
- [4] CMS Collaboration, “The CMS experiment at the CERN LHC”, *JINST* 3 (2008) S08004.
doi:10.1088/1748-0221/3/08/S08004.
- [5] Y. Gao, A.V. Gritsan, Z. Guo, K. Melnikov, M. Schulze, and N.V. Tran, “Spin determination of single-produced resonances at hadron colliders”, *Phys. Rev. D*, 81:075022, 2010.
arXiv:1001.3396
- [6] A.L. Read, “Presentation of search results: the CLs technique”, *Journal of Physics G: Nuclear and Particle Physics*, 28(10):2693, 2002.
- [7] CMS Collaboration, “Search for a Higgs boson in the decay channel $H \rightarrow ZZ \rightarrow 2\ell 2q$ in pp collisions at $\sqrt{s} = 7$ TeV”, *JHEP* 1204 (2012) 036.
arXiv:1202.1416
- [8] CMS Collaboration, “Search for the standard model Higgs boson in the $H \rightarrow ZZ \rightarrow 2\ell 2\nu$ channel in pp collisions at $\sqrt{s} = 7$ TeV”, *JHEP* 1202 (2012) 040.
arXiv:1202.3478
- [9] CMS Collaboration, “Search for the Higgs boson in the $H \rightarrow ZZ \rightarrow 2\ell 2\nu$ channel in 10 fb^{-1} at 7 and 8 TeV”, CMS-HIG-12-023.